Analytical Methods

Accepted Manuscript

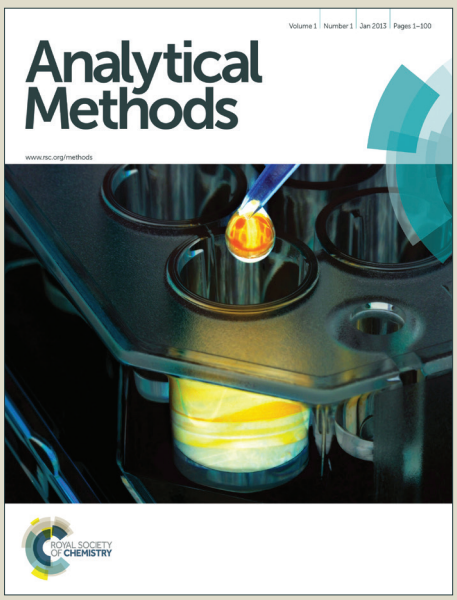

ROYAL SOCIETY OF CHEMISTRY

www.rsc.org/methods

Journal Name

ARTICLE

Digital videometrics analysis for kinetic determination of dopamine in the presence of ascorbic acid based on formation of silver nanoparticles

Received 00th January 20xx,
Accepted 00th January 20xx

DOI: 10.1039/x0xx00000x

www.rsc.org/

Bahram Hemmateenejad,*Fatemeh Shakerizadeh-Shirazi, Sahar Heidari and Arezoo Shahrivar-kevishahi

A simple, cost-effective and rapid method for visual detection of dopamine (DA) and ascorbic acid (AsA) based on the video-image analysis has been developed. The method is based on the formation of silver nanoparticles by reaction of dopamine and/or ascorbic acid with silver nitrate. The video of produced brown color during the reaction was recorded and then the framed images were extracted. Changes in the red, blue and green (RGB) elements of the images as function of time produced kinetic profiles, which were very similar to spectrophotometric study. By fix-time analysis of the kinetic profiles, linear calibration curves were obtained for dopamine and ascorbic acid in the concentration ranges of 4.95 $\times 10^{-6}$–2.38×10^{-5}M and 9.80 $\times 10^{-6}$ –7.63$\times$ 10^{-5} M, with detection limits of 2.5 $\times 10^{-6}$ M and 3.10 $\times 10^{-6}$ M, respectively. Then the imaging-based kinetic profiles were used for multicomponent analysis based on partial least squares (PLS) and principal component analysis-artificial neural network (PC-ANN) models. This is the first attempt to use image analysis for the kinetic determination of dopamine in the presence of ascorbic acid with the aid of chemometrics methods. In this manner, accurate determination of dopamine in the presence of ascorbic acid using a very simple instrumentation was achieved. The root mean square error for estimation of dopamine in the synthetic binary mixtures was about 6%.

Introduction

Over the years, the applications of digital image analysis are progressively growing through all areas of science and industry .[1,2,3] In this method, in addition to experimental data, images of supporting substrate or the colorful solutions can be saved in a computer and subsequent analysis with appropriate programs. In contrast to UV-vis spectroscopy, the cost and time of analysis could be considerably decreased with this approach.[4] In this regards, steady state colorimetric measurements have been increasingly emerged in analytical chemistry. After reaction development of analyte with reagent, the photographs are taken from the solutions or solid supports. The extracted color values using different color spaces (e.g., RGB space) are then correlated with analyte concentration. This type of measurement is analogous to the single wavelength spectrophotometric measurement. Previously, we used image analysis for determination of heparin[5] and for determination of solution bulk properties such as solvent empirical polarity scale (E_T30).[6]

A main drawback of the image analysis is lack of selectivity. So, separation of the analytes by thin-layer chromatography (TLC) followed by image analysis has been achieved for selective and simultaneous determinations.[7,8] However, using a single analytical method with high degree of selectivity is preferred. Here, we used the kinetic aspect of analytical chemistry for increasing the selectivity of the imaging method. By recording the kinetic of color development of the reaction by a digital video, it would be possible to drive the kinetic curve. If analytes in the samples have different kinetic characteristics, simultaneous multicomponent determinations can be done by chemometrics analysis of the kinetic curves.[9]

When the analytes react with a common reagent but with different reaction rates, several analytes can be simultaneously analyzed using the kinetic methodology.[10] This type of analysis can be enhanced significantly by chemometrics procedures.[11-13] Simple analytical methods aided by chemometrics methods based on factor analysis and artificial intelligence, including principal component regression (PCR), partial least squares (PLS) and artificial neural networks (ANNs), have been applied effectively for multicomponent kinetic determinations.[14-19] The influences of the analyte–analyte interaction, the synergistic effect (non-additivity of reaction rates), the multi-step process and any other indefinite nonlinearity can be removed or decreased by these methods.

Through the last decades, using of neural networks in chemometrics has increased.[20] Artificial neural networks (ANN) are flexible nonlinear computational tools and appropriate to the significant practical applications. In multivariate calibration problems excellent results can be obtained using ANN. [21-23]

[a] Department of Chemistry, Shiraz University, Shiraz, Iran

Dopamine (DA), is an important biological molecule, which is found mostly in the central nervous system of mammalians. It can be used as a marker for detection of some diseases in humans such as Parkinson, epilepsy and senile dementia. [24,25] However, measurement of the level of DA in biological fluids usually is associated with the interfering effects of the active species like ascorbic acid (AsA). Therefore, development of selective and sensitive method for simultaneous determination of DA and AsA is extremely required for analytical applications and medical diagnoses. Many methods such as spectrometry, [26] chromatography,[27] capillary electrophoresis[28] and fluorimetry[29] have been reported to detect DA. Nevertheless, there is a demand for simple, fast and cost effective analytical methods for selective analysis of DA in the presence of AsA.

In this research a new method for determination of the DA in the presence of AsA is introduced. The method is based on the videometric monitoring of the formation of silver nanoparticles using DA.[30] The recorded videos were converted to kinetic curves, which followed by chemometrics analysis using PLS and ANN. These multivariate calibration methods correlated the color values with analyte's concentration in linear and nonlinear manners, respectively.

Experimental

Reagents

Dopamine (DA), ascorbic acid (AsA), silver nitrate and polyvinyl pyrrolidone (PVP; average molwt 10,000) were obtained from Merck chemical company. All other common laboratory chemicals were of the best grade available and were used without further purification. Stock solutions of $AgNO_3$ (0.01 M) were prepared by dissolving desired amount of $AgNO_3$ in deionized water. A stock solution of polyvinyl pyrrolidone (PVP) (0.40 g L^{-1}) was prepared daily by dissolving 0.01 g ofPVP in water and diluting to 25 mL. Fresh 0.05 M solution of DA and AsA were prepared daily by dissolving the reagent in deionized water.Deionized water was used throughout the experiments.

Procedure

The reaction solution was consisted of 0.7 mL of PVP 0.4 (g L^{-1}), 1.0 mL of NaOH 0.001 M, different amounts of dopamine and ascorbic acid and 1.0 mL of $AgNO_3$ 0.01 M. They were added in the same order as above to a 5.0-mL volumetric flask and then diluted to the mark. The resulting solutions were mixed slowly and then were transferred into a spectrophotometric cell of inner volume of 1.0 mL and 1.0 cm optical path length. The videos of solutions in the cells were recorded by a camera. It is worth stressing that the order of the addition of the reagents is very essential. Changing the reagent addition order caused the silver nanoparticles to be not stabilized by PVP, so the reduced colloidal stability resulted in rapid formation of silver or silver oxide precipitate. In order to obtain the high quality and reproducible images, a radiation source equipment composed of a two-dimensional array of LED lamps with the capability of producing red, green and blue light was constructed. The lamps can also emit the binary or ternary combination of red, green and blue radiance. In our work, the white source, generated from the mixture of red, green and blue lights, was used as source. The lamps, which were covered with a flexi glass sheet, were put in cabinet. To lower the refraction of the lamps radiation from the different parts of cabinet, the inside cabinet body is coated by black paint. The cells were placed in front of the radiation source. A SONY-H5 digital camera with the capability of taking images with 7.2 Mega pixel resolutions was used and fixed in the front of the cells. The employed camera has different modes of an imaging system. Any mode has a special characteristic; in this work, the auto-adjustment mode and macrophotography, which is close-up photography, were used. The considered reaction was followed in a cell during 7 min.

Table 1 Concentrations of dopamine and ascorbic acid in standard solutions of calibration and prediction sets

Calibration set			Prediction set		
No	Dopamine (μM)	Ascorbic Acid (μM)	No	Dopamine (μM)	Ascorbic Acid (μM)
C1	5.0	30.0	P1	9.0	40.0
C2	5.0	42.0	P2	12.0	20.0
C3	5.0	65.0	P3	12.0	30.0
C4	7.0	25.0	P4	15.0	40.0
C5	7.0	35.0	P5	20.0	42.0
C6	7.0	44.0	P6	24.0	25.0
C7	7.0	60.0	P7	12.0	65.0
CC	10.0	42.0	P8	18.0	49.0
C9	10.0	58.0	P9	22.0	35.0
C10	13.5	35.0	P10	22.0	44.0
C11	15.0	20.0	P11	24.0	47.0
C12	15.0	47.0			
C13	20.0	53.0			
C14	20.0	58.0			
C15	22.0	55.0			
C16	22.0	65.0			
C17	24.0	20.0			
C18	24.0	65.0			

In multivariate calibration, standard solutions of mixtures of analytes are necessary. Here, binary mixtures of DA and AsA were prepared. The training set, composed of 18 binary standard solutions (Table 1), was used to make calibration models between the kinetic curves of the mixtures and concentration of DA. The test solutions (11 standard binarymixtures, Table 1) were used to evaluate the quality of

the models obtained in the training step. The concentrations of DA and AsA in the mixtures were in the micromolar range (in the linear range of the individual calibration curves) and were selected randomly in both sets.

Data analysis

The recorded video of each solution, saved in MPG format, was loaded into computer using KMplayer software version 3.6.0.87. Then, they were converted to the framed images using a graphical user interface (GUI) routine written in MATLAB (Mathwork Inc., version 2011). It is worth to notice that the results from this MATLAB function were compared to the software of free video to JPG Converter v.5.0.4 build 1228 (freestudio/www.DVDVIDEOSOFT.com) and the results were found to be similar to each other. With this graphical user interface, user can run the program in two modes; original images or background subtracted images.

The recorded movie of each solution during 7 min reaction is converted to 10545 frames. So, each frame corresponds to 0.04 S. Each image pixel is converted to R, G and B values and then the averaged values of these color indices over all pixels are calculated ($\overline{R}, \overline{G}$ and $\overline{B}$, respectively). The same is done for the background movie (taken from blank solution). The ratios of the color values of the samples to those of the background ($\overline{R}_{s/b}$, $\overline{G}_{s/b}$ and $\overline{B}_{s/b}$, respectively) are chosen as analytical signal. Thus, for each image a row vector of length of 3 (i.e., $[\overline{R}_{s/b}\overline{G}_{s/b}\overline{B}_{s/b}]$) is provided. By staking the color value vectors of all frames of a video (collected over recording time) under each other a kinetic data matrix of size (10545×3) is obtained for each sample.Consequently, having nc samples in the calibration set and np samples in the prediction, their data sets can be arranged into three-way data arrays of Dc and Dp with the size of (nc×10545×3) and (np×10545×3), respectively. However, since first order multivaritate calibration methods need two-way arrays of data, the three-way data sets are unfolded to two-way data so that each row are containing (10545×3) variables.

The kinetic data were processed by PLS and back-propagation trained ANN as linear and nonlinear methods, respectively. The NIPALS-based PLS-1 regression implemented leave-one-out cross-validation to select the optimum number of latent variables. The structure of the network is comprised of three node layers: an input layer, a hidden layer and an output layer. To avoid feeding of ANN with large number of input variables, the data matrix was factor analyzed before its introduction into the network and the PC-ANN model was run.[20] The adjustment of the weights was done using back-propagation learning algorithm.

For PLS analysis, the PLS-toolbox developed by Eigen-vector company was used. The ANN modeling performed utilizing neural network tool-box of MATLAB.

Results and discussion

In this work, a new and simple method for determination of DA in the presence of AsA is proposed using video-image analysis. The chemical system in this study consisted of an aqueous $AgNO_3$ solution and poly vinyl pyrrolidone (PVP), as stabilizer, in an alkaline medium.[30] The chemicals DA and AsA act as effective reducing agents for reduction of silver ions (Ag^+) to the Ag-NPs without adding seeds. As the focus of our research is on the video image analysis and to compare it with conventional spectrophotometric method, the optimized experimental parameters that reported previously by a spectrophotometric method were used.[30] Protective agents or stabilizers play an important role in stabilizing the nanoparticle colloidal metals from agglomeration as indicated by the two essential modes: electrostatic and steric stabilization.[30] In this study, for preventing silver nanoparticles agglomeration, PVP (0.06 g L^{-1}) was selected as stabilizers according to the previous paper.[30] The analytes have a dihydroxyphenyl group which can lose H^+ during oxidation, therefore, the effect of NaOH concentration on Ag^+ reduction by the analytes is expected. A 0.2 m MNaOH solution was added to give sufficient alkalinity because buffered conditions failed to produce silver nanoparticles.

When reducing agents are not added, there is no absorption peak in visible region (380–700 nm). However, when DA and AsA, acting as reducing agents, are added, silver ions are reduced to silver nanoparticles and consequently the absorbance characteristic of the surface plasmon of the Ag-NPs is detected. Fig. 1 shows the absorption spectra and image of the Ag nanoparticles solution that was produced by addition of the DA to silver nitrate solution. Fig. 2 shows change in the R, G and B color value of Ag+ solution vs. time after addition of DA and AsA. As it is obvious, the reaction of silver ions with AsA is faster than that with DA and it is practically finished within 3 min. It is clear from Fig.2a that the color value B is more affected when color of the reaction in monitored by reaction progress. So, in the next, B color value was considered as analytical signal.

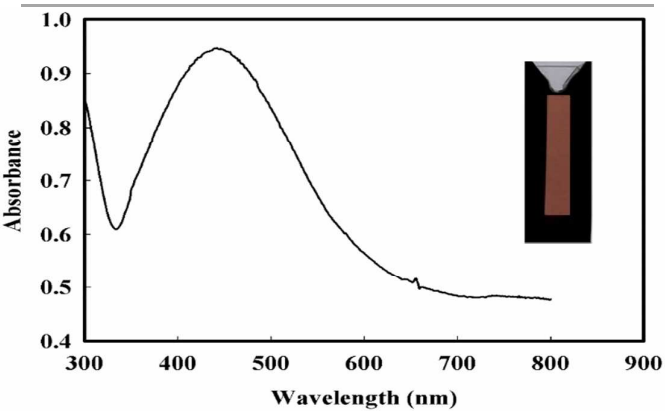

Fig. 1. Absorbance spectrum and image of the Ag-NPs solution formed by addition of 2.0×10^{-5} M DA to silver nitrate under the optimum conditions: AgNO3 (2×10^{-3} M), PVP (0.06 g L^{-1}) and NaOH (0.2 mM).

Univariate calibration

Similar to all multivariate calibration-based analytical methods, the first step is to determine the individual linear dynamic ranges of each analyte, or in other words, is to find the relation between the color intensity and concentration of the studied analytes. This was achieved by plotting the B color value of each solution image after 6 min of the reaction progress against the analyte concentration.

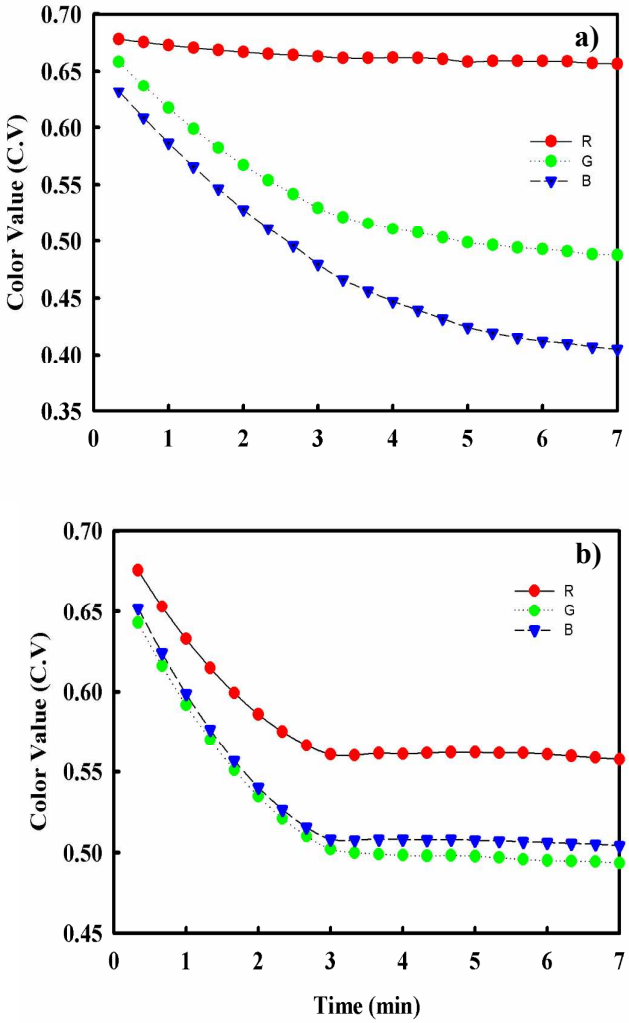

Fig. 2. Kinetic curves corresponding to the color value changes of the DA (23.8μM) (a) and AsA (23.8μM) (b), representing growth of Ag-NPs. Conditions: $AgNO_3$ (2×10^{-3} M), PVP (0.06 g L^{-1}), NaOH (0.2 mM).

The analytical appraisal of the individual calibration curves are shown in Table 2. For comparison, the previously found values by spectrophotometric method are also shown in this Table. Under the optimum condition, the calibration curves were linear in the ranges of 4.95×10^{-6}–2.38×10^{-5} M and 9.80×10^{-6} – 7.63×10^{-5} M for DA and AsA, respectively that are approximately similar to those of the previous spectrophotometric method. The detection limits obtained by videometric method are also comparable with those obtained by spectroscopic method.

Table 2 Analytical appraisals for univariate calibration of the individual analytes

Method	Analyte	Linear range (μM)	R^2	D.L. (μM)	RSD%(n=3)
Videometry	Dopamine	4.95-23.80	0.980	2.50	3.40
	Ascorbic acid	9.80-76.30	0.987	3.10	4.50
Spectrophotometry	Dopamine	3.20-20.00	0.997	1.20	3.20-4.50
	Ascorbic acid	2.00-48.00	0.992	1.10	2.50-3.80

Multivariate calibration

In the previous section, it was shown that dopamine and ascorbic acid can be determined individually by image detection employing simple univariate calibration. These two analytes normally coexist in real biological fluids, so the improvement of a selective and sensitive method for the determination of DA coexisted with AsA is very necessary for clinical applications. Kinetic approaches have been extensively utilized for the synchronous determination of multi-component mixtures because of the accessibility of computerized information acquisition systems and the improvement of effective mathematical treatments for analyzing the recorded data.[30] Chemometrics approaches, e.g., principal component regression (PCR), partial least squares regression (PLS) and artificial neural networks (ANN) as recognized multivariate calibration methods are broadly utilized over the last decades for the concurrent determination of analytes in mixtures by means of kinetic-spectrophotometric methodology.[31-33] Using of analytical methods combined with multivariate calibration can be considered a promising, faster, direct and relatively less expensive alternative for multicomponent analysis of mixtures. Based on the reported linear ranges in the univariate calibration, standard binary mixtures of the analytes (18 calibration samples and 11 prediction samples) were provided (Table 1). As it was explained previously, the videos of Ag^+ solution after reaction with the binary mixture of the analytes were recorded according to the procedure described in the experimental section and were converted to the corresponding images. Then the color values of each solution

were taken as analytical signals. The framed images and the corresponding kinetic curve of a representative mixture are shown in Fig. 3.

At the first, linear multivariate calibration methods, PLS, were used to estimate dopamine concentration in binary solutions. Therefore, the kinetically recorded color values were used as the input of the PLS-based multivariate calibration methods for the determination of dopamine in their mixtures. It should be noted that the multivariate calibration model of AsA was not of high statistical quality and hence the results of this analyte are not discussed. So, the focus is on the determination of DA in the presence of AsA. The PLS was performed in the PLS-1 fashion. A major step in the PLS model development is finding the correct

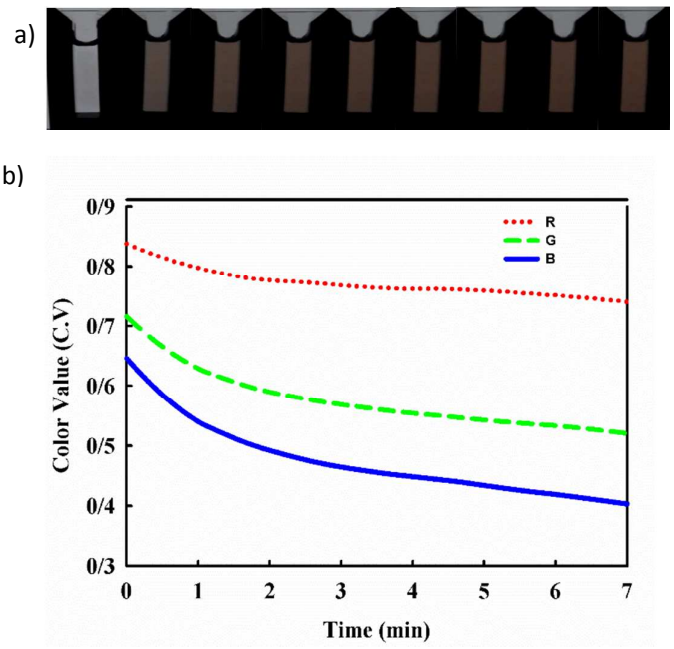

Fig. 3. (a)Time-dependent Photographs and (b) Kinetic curves corresponding to the color value changes of Ag^{+} solution after reaction with a binary mixture of dopamine (13.5 µM) and ascorbic acid (13.5 µM).

number of latent variables in which the model has sufficient performance to predict the concentration of the analyte not only from the internal data (calibration data) but also from external sources (prediction data). Cross-validation, as a standard procedure that validates both the predictive and generalization ability of the models[34] was used to select the optimal number of PLS factors. It was observed that 2 latent variables were optimum. The resulted models were used to predict the concentrations of the analytes in the prediction samples. It should be noted that the prediction samples did not contribute to PLS model development.

Some statistical parameters, including root mean square errors of cross-validation and prediction (RMSCV and RMSP, respectively), the square of correlation coefficient for cross validation and for prediction set (R^2_{CV} and R^2_{P}), were used to estimate the performance of the resulted models. The statistical parameters of the PLS models developed for determination of dopamine are summarized in Table 3. The plot of the predicted values against the experimental values of DA concentration and the corresponding residual plots are given in Fig. 4. The predicted values are given in the supplementary section Table S1. As seen, the obtained model is associated with almost large errors. Moreover, the residual plots represent a systematic shape. These observations suggest that PLS is not an adequate model for the processing of the video data in the studied system. Thus, using of ANN as a nonlinear multivariate calibration method was suggested.

Over the last decades, the use of neural networks in chemometrics has been increased.[35,36] Artificial neural networks (ANN) are a type of nonlinear processing tools that are

Table 3 Statistical parameters for the optimized PLS and ANN models in determination of DA

Model	Calibration				Prediction		
	$RMSE_C$	RMS_c(%)	R^2	RMS_{CV} (%)	$RMSE_P$	RMS_p(%)	R^2
PLS	1.38	10.43	0.96	12.54	1.05	5.83	0.97
ANN	0.75	5.65	0.99	7.05	1.06	6.13	0.98
ANN-Chance effect	14.7		0.31	19.53	17.27		0.24

appropriate for an extensive variety of applications. ANN can be trained to resolve definite problems using a teaching process and data sampling. It is possible to get great results in multivariate calibration issues using ANN. [22] Application of ANN model with data pretreatment strategy, for example, normalization[23] and principal component analysis (PC-ANN) in various kinetic conditions have been reported.[37,38] The most common network architecture is multilayer feed-forward networks with the back-propagation learning algorithm.[39,40]

The number of adjustable parameters (weights) in ANN depends on the number of variables in the input layer. Previous studies proposed decreasing the data volume before using ANN for nonlinear multivariate calibration as a preprocessing step.[41] Thus, we applied PCA, as a preprocessing method, on the color intensity data matrices obtained from the kinetic monitoring of mixtures of DA and AsA. The variables of ANN input layer were the calculated PCs. We would like to emphasis that reduction of data dimensionality by PCA increases the numerical stability of the model and in the same time it generate orthogonal variables.[42]

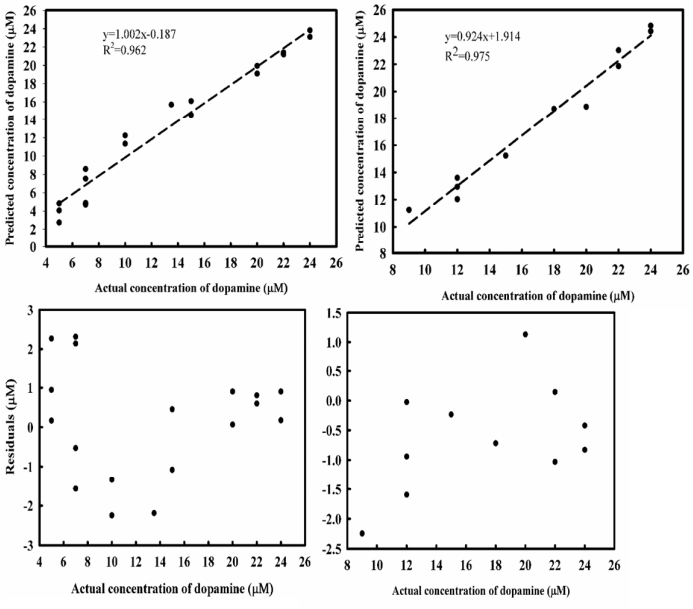

Fig.4. Plot of the predicted concentrations against the experimental values (left) and the corresponding residual plots (right) for the calibration (top) and prediction (bottom) sets obtained by PLS for DA.

The optimum number of variables in the input layer was selected using cross-validation. The RSEP% of cross-validation for each analyte reached to a minimum at number of PCs of 2. The optimum number of nodes in the hidden layer was obtained by trying number of nodes of 1-10. Random correlation because of random initialization of the weights was avoided by repeating each ANN model five times. The least RSEP% value obtained for number of hidden units of 1. All other parameters of ANN with back-propagation learning algorithm including number of iterations, momentum, learning rate and transfer functions were optimized using minimum RSEP% values of cross-validation during the training process. The parameters of the optimized ANN model are summarized in Table 4.

For the constructed model, four general statistical parameters were selected to evaluate the prediction ability of the model. For this case, the predicted concentrations of dopamine in each sample in prediction and calibration sets were compared with the actual concentrations. The prediction results are given in the supplementary materials Table S2 and the statistical parameters are summarized in Table 3. The high correlation coefficients (0.99 for the calibration and 0.98 for the prediction set) and low average relative errors (5.65% for the calibration set and 6.13% for the prediction set) reveal the capability of the obtained model for the prediction of dopamine concentration. It should be noted that leave-one-out cross validation was run at five different weight initialization trials. Also, the prediction set samples did not have contribution in the network training and the best network was selected using cross-validation.

Table 4 Artificial Neural Network Specifications and Parameters

Parameter	Data
Number of input nodes	2
Number of hidden nodes	1
Learning rate	0:00:09
Momentum	0.1
Gradient	1.56×10^{-6}
Input -layer transfer function	Linear
Hidden- layer transfer function	Sigmoid
Output -layer transfer function	Linear

ANN models are prone to chance correlation. In order to further evaluate the ANN model obtained in this work, the chance effect was also checked. The performance of the designed networks was examined to carry out multivariate calibration by permuting output vector (concentration of DA). Detailed results from these experiments are given in the last row of Table 3. The root mean square errors are worse for the calibration and prediction setsconfirming that the obtained model is not chancy.

The plots for the predicted values against the experimental values and the corresponding residual plots obtained by ANN are depicted in Fig. 5. The data are distributed around a straight line with slope and intercept close to the ideal values (1 and 0, respectively). An interesting point is the homogenous scattering of residuals for both training and predictionsets and they do not show structured distribution. The obtained results by ANN confirm that the suggested model is not only optimum for self-prediction but it can also accurately predict the dopamine concentration of the external samples.

Finally, it should be noted that construction of multivariate calibration models for ascorbic acid by either PLS or ANN did not results in meaningful calibration models. All constructed models for this analysis were associated with high level of prediction error. So, the results of ascorbic acid analysis were not included in this work. However, this work represents a significant improvement in analysis of dopamine in the presence of ascorbic acid as ever interfering species.

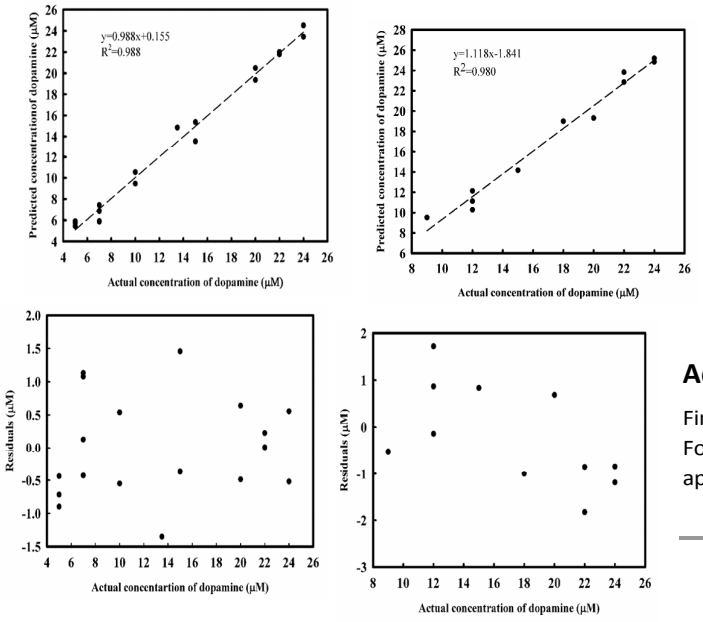

Fig. 5. Plot of the predicted concentrations against the experimental values (left) and the corresponding residual plots (right) for the calibration (top) and prediction (bottom) sets obtained by ANN for DA.

Analytical application

To demonstrate the potential application of our proposed method for DA detection in the presence of AsA in real samples, recovery experiments were carried out by analyzing the spiked human serum samples (Table 5). Different concentrations of each compounds were spiked to a 100-fold diluted serum samples. The recoveries were evaluated, assuming zero level of DA and AsA in serum as it was declared by the blood transplantation center of Shiraz. The results shown in Table 5 suggest satisfactory recovery and precision of the proposed method.

Conclusions

In this work, we have explored analytical strategy and the chemometrics interpretation of the results for the determination of dopamine in the presence of ascorbic acid in synthetic samples by the new kinetic–video analysis method. The suggested technique was reliant on the reduction of Ag+ by the analyte to produce silver nanoparticles. The kinetics of the formation of silver nanoparticles by DA and AsA pursued by video analysis showed that the proposed strategy is acceptable for the determination of DA in the presence of AsA. PLS models did not result in suitable calibration model. However, PC-ANN resulted in accurate prediction results.

It is worthy to stress that the methods described here would also be valuable for the analysis of different components by adjusting the optimum conditions. This achievable study indicated very attractive results using just a simple CCD camera and chemometrics methods in the research center for desirable observation. We are sure it will offer new trends in analytical chemistry. Based on these and our previous results, we hope to see in the future the improvement of low-cost spectral based imaging tools with working very close to more expensive and complex multispectral devices.

Acknowledgements

Financial support of this project by Iran National Elites Foundation and Shiraz University Research Council is highly appreciated.

Table 5. Determination of DA and AA in human serum as a real sample

	Added		Found	Recovery(%)
Sample	Dopamine (μM)	Ascorbic Acid (μM)	Dopamine (μM)	
1	5.4	11.1	5.7	105.5
2	7.2	19	6.9	95.9
3	11.0	34.5	9.9	90.0
4	15.7	50.9	16.2	103.2
5	20.5	69	22.5	109.7

References

1 A. Abbaspour, F. Norouz-Sarvestani and E. Mirahmadi, *J. Iran. Chem. Soc*., 2012, **9**, 383.
2 Y. Liu, J. Ling and C.Z. Huang, *ChemCommun*., 2011, **47**, 8121.
3 J. Hao, B. Xiong, X. Cheng, Y. He and E.S. Yeung, *Anal. Chem.*, 2014, **86**, 4663.
4 M. Kompany-Zareh, H. Tavallali, N. Shakernasab, M. Khoshkam and E. Shamsdin, *Reac. Kinet. Mech. Cat*., 2012, **107**, 49.
5 B. Hemmateenejad, S. Dorostkar, F. Shakerizadeh-Shirazi and M. Shamsipur, *Analyst*, 2013, **138**, 4830.
6 F. Shakerizadeh-Shirazi, B. Hemmateenejad and A. M. Mehranpour, *Anal. Methods*., 2013, **5** , 891.
7 B. Hemmateenejad, N. Mobaraki, F. Shakerizadeh-Shirazi and R. Miri, *Analyst*, 2010, **135**, 1747.
8 B. Hemmateenejad, M. Akhond, Z. Mohammadpour and N. Mobaraki, *Anal. Methods*., 2012, **4**, 933.
9 J. Tashkhourian, M.R. Hormozi-Nezhad and J. Khodaveisi, *Spectrochim. Acta A*., 2011, **82**, 25.
10 D. Perez-Bendito, *Analyst*, 1990, **115**, 689.
11 S.R. Crouch, *Anal. Chim. Acta* ., 1993, **283**, 453.
12 M. Otto, *Analyst*, 1990, **115**, 685.
13 T.F. Cullen and S.R. Crouch, *Mikrochim. Acta*., 1997, **126**, 1.
14 G. Absalan and M. Nekoeinia, *Anal. Chim. Acta*., 2005, **531**, 293.
15 Y. Ni, P. Qiuand S. Kokot, *Anal. Chim. Acta*., 2004, **516**, 7.

16 Y. Ni, C. Huang and S. Kokot, *Anal. Chim. Acta* ., 2003, **480**, 53.
17 A. Safavi, O. Moradlou and S. Maesum, *Talanta*, 2004, **62**, 51.
18 A. Safavi, H. Abdollahi and M.R. HormoziNezhad, *Talanta*, 2003, **59**, 515.
19 I.A. Pettas and M.I. Karayannis, *Anal. Chim. Acta*., 2003, **491**, 219.
20 F. Marini, R. Bucci, A.L. Magri and A.D. Magri, *Microchim. J.* , 2008, **88** , 178.
21 P.J. Gemperline, J.R. Long and V.G. Gregoriou, *Anal. Chem*., 1991, **63**, 2313.
22 C. Borggard and H.H. Thodberg, *Anal. Chem*., 1992, **64**, 545.
23 P. Geladi and B.R. Kowalski, *Anal. Chim. Acta*., 1986, **185**, 19.
24 B. Ge, Y. Tan, Q. Xie, M. Ma and S. Yao, *Sens. Actuators, B: Chem*., 2009, **137**, 547.
25 R.D. áO'Neill, *Analyst*, 1994, **119**, 767.
26 L. Guo, Y. Zhang and Q.Li, *Anal Sci.,*2009, **25**, 1451.
27 C.L. Guan, J. Ouyang, Q.L. Li, B.H. Liu and W.R.G. Baeyens, *Talanta*., 2000, **50**, 1197.
28 R. Zhu and W.T. Kok, *Anal. Chem*., 1997,**69**, 4010.
29 H. Nohta, T. Yukizawa, Y. Ohkura, M. Yoshimura, J. Ishida and M. Yamaguchi, *Anal. Chim. Acta*., 1997, **344**, 233.
30 M.R. HormoziNezhad, J. Tashkhourian, J. Khodaveisic and M.R. Khoshi, *Anal. Methods*., 2010, **2**, 1263.
31 A. Afkhami, N. Sarlak and A. R. Zarei, *Talanta*, 2007, **71**, 893.
32 Y. Ni, Y. Wang and S. Kokot, *Food Chem*., 2008, **109**, 431.
33 M. Chamsaz, A. Safavi and J. Fadaee, *Anal. Chim. Acta*., 2007, **603**, 140.
34 R.G. Brereton, *Chemometrics: Data Analysis for the Laboratory and Chemical Plant*, John Wiley &Sons., 2003.
35 G. Kateman, *Chemometr. Intell. Lab. Syst*., 1993, **19**, 135.
36 J.R.M. Smits, W.J. Melssen, L.M.C. Buydens and G. Kateman, *Chemometr. Intell. Lab. Syst*., 1994, **22**, 165.
37 M. Blanco, J. Coello, H. Iturriaga, S. Maspoch and M. Redon, *Anal. Chem*., 1995, **67**, 4477.
38 M. Blanco, J. Coello, H. Iturriaga, S. Maspoch, M. Redón and N. Villegas, *Analyst*, 1996, **121**, 395.
39 J. Gasteiger and J. Zupan, *Angew. Chem. Int. Ed*., 1993, **32**, 503.
40 F. Despagne and D. Luc Massart, *Analyst*, 1998, **123**, 157R.
41 P.J. Gemperline, *Chemometr. Intell. Lab. Syst*., 1992, **15**, 115.
42 S. Sekulic, M.B. Seasholtz, Z. Wang, B.R. Kowalski, S.E. Lee and B.R. Holt, *Anal. Chem*., 1993, 65, 835A.